

# Blending and White Spirit Permeation Properties of the Blends of Modified Polyamide and Ethylene Vinyl Alcohol with Varying Vinyl Alcohol Contents

Jen-Taut Yeh,<sup>1,2</sup> Heng-Yi Chen,<sup>2</sup> Fang-Chang Tsai<sup>2</sup>

<sup>1</sup>Faculty of Chemistry and Material Science, HuBei University, Wuhan, People's Republic of China

<sup>2</sup>Department and Graduate School of Polymer Engineering, National Taiwan University of Science and Technology, Taipei 106, Taiwan

Received 12 April 2005; accepted 31 January 2006

DOI 10.1002/app.24425

Published online in Wiley InterScience (www.interscience.wiley.com).

**ABSTRACT:** The blending and white spirit permeation properties of the MPAEVOH blends of modified polyamide (MPA) and ethylene vinyl alcohol copolymer (EVOH) were systematically investigated in this study. Three types of EVOHs with varying vinyl alcohol contents were used to prepare the MPAEVOH resins by melt blending them with the MPA resin, respectively. The peak melting temperatures and percentage crystallinity ( $W_c$ ) values of the EVOH specimens increase significantly as their vinyl alcohol contents increase. The X-ray diffraction patterns of the melt-crystallized EVOH crystals transform from monoclinic to orthorhombic lattice as their vinyl alcohol contents are equal to or less than 56 wt %. After blending EVOH in MPA resins, the main melting endotherms and characteristic X-ray diffraction patterns of both monoclinic and orthorhombic lattices of EVOH crystals originally present in

MPAEVOH specimens almost disappear completely, when the weight ratios of MPA to EVOH are equal to or greater than 4. The free-volume properties and white spirit permeation rates of the EVOH specimens reduce significantly as their vinyl alcohol contents increase. A noticeable "negative deviation" was found on the plots of white spirit permeation rates, annihilation intensity ( $I_3$ ), and/or fractional free-volume ( $F_v$ ) versus MPA contents as the MPA contents of each MPAEVOH sample series reach about 80 wt %. Possible reasons accounting for these interesting blending and barrier properties of MPAEVOH specimens are discussed. © 2006 Wiley Periodicals, Inc. *J Appl Polym Sci* 102: 1224–1233, 2006

**Key words:** blending; barrier; ethylene vinyl alcohol copolymer; modified polyamide; free-volume

## INTRODUCTION

It is well known that many hydrocarbon solvents (e.g., xylene, toluene, white spirit, etc.) are commonly available products that easily permeate polyethylene (PE) containers; such permeation results in pollution, safety and health problems. For instance, about 65% of the filled white spirit permeated out of 1 mm thick PE bottle in 6 months at 40°C,<sup>1</sup> wherein the white spirit is widely used as the paint thinner around the world. A "laminar-blend-blow-molding process" forms a layered structure containing numerous discontinuous, overlapping platelets of barrier resins, such as polyamide (PA) and/or ethylene vinyl alcohol copolymers (EVOH), in a PE matrix, which is one of well proven barrier technologies to enhance the resistance of PE containers to hydrocarbon permeation.<sup>2–14</sup> These heterogeneous laminar blends exhibit significantly higher permeation barrier properties than conventional homogeneous blends associated with uniform dispersed PA and/or EVOH droplets within the PE matrix.<sup>5–18</sup>

Our investigation<sup>1</sup> found that the barrier improvement of white spirit permeation of PE bottles can be improved by more than 360 times after blending proper compositions of modified polyamide (MPA) in PE matrix during the blow-molding process. The white spirit composed of more than 100 hydrocarbon compounds with 5–12 carbon atoms by GC analysis. The main components present in the white spirit are hydrocarbon components with 8–9 carbon atoms. On the basis of these premises, it is reasonable to suggest that the relatively nonpolar hydrocarbon components present in the white spirit can easily permeate PE bottles during the permeation tests. In contrast, after blending the MPA barrier resins in PE matrix, the nonpolar hydrocarbon components present in the white spirit were significantly blocked by the MPA laminar structures and allowed restricted permeation during the permeation tests. In contrast to MPA, EVOH, known for its excellent transparency, oil resistance, and outstanding barrier properties against nonpolar gas and solvent permeations, is recognized as an even better barrier material in packing applications. Our recent study<sup>13</sup> indicated that much better gasoline permeation resistance was obtained after blending proper amounts of EVOH in

Correspondence to: J.-T. Yeh (jyeh@tx.ntust.edu.tw).

MPA during the blow-molding processes of PE/blends of MPA and ethylene vinyl alcohol (MPAEVOH) bottles. For instance, by using the optimum MPAEVOH composition, the gasoline permeation rate of PE/MPAEVOH bottle is about 450 and three times slower than that of the PE and PE/MPA bottles, respectively. However, as far as we know, the influence of the vinyl alcohol contents of EVOH resins on nonpolar solvent permeation properties of the laminar PE/MPAEVOH containers have never been reported. The main objective of this study is to investigate and compare the white spirit permeation properties and mechanisms of MPAEVOH, wherein three kinds of EVOH resins with varying vinyl alcohol contents were used to prepare the MPAEVOH resins by blending them with the MPA resin, respectively.

## EXPERIMENTAL

### Materials and sample preparation

The PA and compatibilizer precursor (CP) used in this study were obtained from Formosa Chemicals and Fiber Corp., Taiwan, wherein PA is nylon 6 with a trade name of Sunylon 6N and CP is a 40% zinc-neutralized ethylene/acrylic acid (95 : 5) copolymer. The MPA resin was prepared by reactive extrusion of the melt blending of CP and PA. The polyethylene (HDPE Taisox 9003), EVOHs with varying vinyl alcohol contents and antioxidant (Irganox B225) used in this study were obtained from Formosa Plastic Corp. (Taipei, Taiwan), Kuraray Corp. (Osaka, Japan) and Ciba-Geigy Corp. (Basel, Switzerland), respectively. For convenience, the EVOH resins with 32, 44, and 48 wt % ethylene contents will be referred to as EVOH32, EVOH44, and EVOH48 resins, respectively, in the following discussion. The physical properties of MPA and EVOH with varying vinyl alcohol contents resins are summarized in Table I.

Before melt blending, PA was dried at 80°C for 16 h, while EVOH and CP were dried at 60°C for 16 h in a vacuum oven. About 1500 ppm of antioxidant was dry-blended with the dried PA/CP blend of varying weight ratios. The dry-blended PA/CP blends together with antioxidant were then fed into an Ekegai PCM 45 corotating twin-screw extruder to make MPA

**TABLE I**  
The Physical Properties of MPA and EVOH Resins

Samples	MPA	EVOH32	EVOH44	EVOH48
Ethylene content (%)	—	32	44	48
Melt index (g/10 min)	2.4 <sup>a</sup>	4.0 <sup>b</sup>	5.5 <sup>b</sup>	6.5 <sup>b</sup>
Density (g/cm <sup>3</sup> )	1.13	1.19	1.14	1.12
$T_m$ (°C)	220	189	183	163

<sup>a</sup> 230°C/2160 g.

<sup>b</sup> 190°C/2160 g.

**TABLE II**  
The Compositions of MPAEVOH Specimens Prepared in This Study

Specimens <sup>a</sup>	MPA (%)	EVOH (%)
MPA(33%)EVOH(67%)	33.33	66.67
MPA(67%)EVOH(33%)	66.67	33.33
MPA(80%)EVOH(20%)	80.00	20.00
MPA(83%)EVOH(17%)	83.33	16.67

<sup>a</sup> The EVOH resins with 32, 44, and 48 wt % ethylene contents are referred to as EVOH32, EVOH44, and EVOH48 resins, respectively.

resin. The extruder was operated at 220°C in the feeding zone and at 240°C towards the extrusion die with a screw speed of 100 rpm. The CP MPA obtained from twin-screw extruder was quenched in cold water at 15°C and cut into the pellet form. Formation of CP-grafted-PA copolymers through the reaction of carboxyl groups of CP with the terminal amine groups of PA has been reported during the preparation of MPA.<sup>5,19</sup> The blends of MPA and EVOH (MPAEVOH) were prepared by melt blending of the MPA and EVOH using a Fure Shuen 40SP-H single-screw extruder. The dried components of MPA/EVOH at varying weight ratios were fed into the single-screw extruder which was operated at 220°C with a screw speed of 400 rpm in the feeding zone and 235°C towards the extrusion die. The extruded MPAEVOH resins were then quenched in cold water at 15°C and cut into the pellet form. The compositions of the three groups of MPAEVOH specimens prepared in this study are summarized in Table II.

### Thermal properties

The thermal properties of EVOH, MPA and MPAEVOH resins were determined using a Du Pont 2010 differential scanning calorimetry (DSC). All scans were carried out at a heating rate of 10°C/min and under flowing nitrogen at a flow rate of 25 mL/min. The instrument was calibrated using pure indium. Samples weighing about 15 and 0.5 mg were placed in standard aluminum sample pans for percentage crystallinity ( $W_c$ ) and melting temperature ( $T_m$ ) measurements, respectively. The heat of fusion for perfect crystal 190 J/g<sup>20</sup> and baselines drawn from 190 to 250°C were used for evaluating the  $W_c$  values of PA or MPA present in MPAEVOH. The  $W_c$  values of EVOH present in MPAEVOH were evaluated using baselines drawn from 160 to 200°C and a perfect heat fusion of 192.3, 215.1, and 229.4 J/g with EVOH32, EVOH44, and EVOH48 calculated using a simple mixing rule.<sup>21</sup> Baselines used in the experiments were adjusted to have the maximum fluctuation less than 0.04 mW over the temperature range of interest. With these baselines, the accuracy for crystallinity determi-

nation is about  $\pm 1\%$  for pure specimens and  $\pm 3\%$  error for blended specimens.

### Free-volume properties

The free-volume characteristics of polymer were determined using a positron annihilation life-time (PAL) instrument equipped with a fast-fast coincidence spectrometer and a  $^{22}\text{Na}$  source that was sandwiched between one layer of hot-pressed film with 1 mm thickness on both sides to ensure complete annihilation of positron in the sample. A short-lived component ( $\tau_1$ ;  $\sim 0.12$  ns), an intermediate-lived component ( $\tau_2$ ;  $\sim 0.35$ – $0.4$  ns), and a long-lived component ( $\tau_3$ ;  $\sim 1.8$ – $2.5$  ns), are the three resolved life-time components obtained, that are attributed to the *para*-positronium (*p*-Ps), free positron, and *ortho*-positronium (*o*-Ps) states, respectively. The longest lifetime component  $\tau_3$  with intensity  $I_3$  is attributed to the pick-off annihilation of the *o*-Ps in the free-volume sites present mainly in the amorphous regions of the polymer matrix.<sup>22</sup> The annihilation of *o*-Ps in the spherical free-volume-cavities can be described by a simple quantum mechanical model, which assumes the *o*-Ps atom to be localized in a spherical potential well with an electron layer of thickness  $\Delta R$ . This model provides the relationship between the radius  $R_f$  of the free-volume hole and the *o*-Ps life-time ( $\tau_3$ ) as follows:<sup>22,23</sup>

$$\frac{1}{\tau_3} = 2 \left[ 1 - \frac{R_f}{R_0} + \frac{1}{2\pi} \sin \left( \frac{2\pi R_f}{R_0} \right) \right] \quad (1)$$

Where  $R_0 = R_f + \Delta R$ , Parameter  $\Delta R$  was determined by fitting the experimental values of  $\tau_3$  obtained for materials of known hole size such as zeolites. The  $\Delta R$  value of 1.66E was used in this study.<sup>24</sup>

The fractional free-volume, defined as the ratio of free-volume to the total volume of polymer, was calculated using following equation.<sup>25,26</sup>

$$F_v = CV_f I_3 \quad (2)$$

where the coefficient  $C$  is a structural constant, one way of calculating  $C$  is from a measurement of the thermal expansion coefficient of the free-volume. The unit of the  $C$  constant is  $\text{\AA}^{-3}$ ,  $I_3$  (%) is the intensity of *o*-Ps life-time, and  $V_f$  ( $\text{\AA}^3$ ) is the mean volume of the free-volume holes calculated using mean radius  $R_f$  obtained as follows:

$$V_f = 4/3\pi R_f^3 \quad (3)$$

### Wide angle X-ray diffraction

The wide angle X-ray diffraction (WAXD) properties of PA, EVOH, MPA and three series of MPAEVOH

specimens were determined using a Siemens D5000D diffractometer equipped with a Ni-filtered Cu K $\alpha$  radiation operated at 40 kV and 100 mA. Each specimen with 2 mm thickness was maintained stationary and scanned in the reflection mode from 5 to 40° at a scanning rate of 5° min<sup>-1</sup>.

### Permeation tests

As shown in our previous study,<sup>6</sup> the solvent permeation mechanisms of PE, PE/PA, and PE/MPA blow-molded bottles were investigated. The solvent permeation rates of PE, PE/PA, and PE/MPA bottles at each temperature initially increase significantly and then slightly with further increase in testing time before reaching the steady state. The steady permeation rate of PE, PE/PA, PE/MPA bottles were plotted versus the testing temperature, which are very close to the average permeation rates obtained by dividing the cumulative weight loss of xylene by the testing time (i.e., 14 days). On the basis of these premises, the permeation rate of the white spirit contained in the bottles is normally evaluated by measuring the weight losses after 14 days. The white spirit permeation properties of MPA, EVOH, and MPAEVOH resins were determined based on their hot-pressed sheets. The dried pellets of MPA, EVOH, and MPAEVOH were hot-pressed into about 2 mm thick sheets and cut into circular of a diameter of 14 cm. The circular MPA, EVOH, and MPAEVOH sheets were sealed as lids on the top of test flasks filled with 250 g of the white spirit. The permeation barrier data were determined by measuring the weight losses of the solvents after placing the flasks at 40°C/60% RH for 14 days on both sides of the circular sheet specimens. The white spirit permeation rate of each of the hot-pressed sheet was estimated based on the average permeation rate of at least three hot-pressed sheet samples. The errors of the values of permeation rates were around  $\pm 10\%$  for the sheets.

## RESULTS AND DISCUSSION

### Thermal properties of MPA, EVOH, and MPAEVOH specimens

Table III summarized the melting temperature and percentage crystallinity ( $W_c$ ) values of MPA, EVOH, CP, and MPAEVOH specimens. Typical melting thermograms of these specimens are summarized in Figure 1, it is interesting to note that the peak melting temperatures and  $W_c$  values of the EVOH specimens increase significantly from 162.9°C and 31.1% to 183.4°C and 37.9% and then to 189.1°C and 40.8% as their vinyl alcohol contents increase from 52 to 56 and then to 68 wt %. In comparison with the EVOH resins, MPA specimen exhibits higher peak melting temperature at around

TABLE III  
Melting Temperature ( $T_m$ ) and Percentage Crystallinity ( $W_c$ ) of MPA, EVOH, and MPAEVOH Specimens

Specimens	EVOH-rich phases			MPA-rich phases			Overall measured $W_c$ (%)	Overall $W_c$ calculated using simple mixing rule (%)
	$T_m$ (°C)	Crystallinity $W_c$ (%)	We calculated using simple mixing rule (%)	$T_m$ (°C)	Crystallinity $W_c$ (%)	Wc calculated using simple mixing rule (%)		
MPA	(92.4) <sup>a</sup>	–	–	220.5	22.4	22.4	22.4	22.4
MPA(83%)EVOH32(17%)	–	0.0	6.8	219.4	24.1	18.7	24.1	25.4
MPA(80%)EVOH32(20%)	–	0.0	8.2	218.5	22.2	17.9	22.2	26.1
MPA(67%)EVOH32(33%)	183.2	1.8	13.6	217.7	16.2	14.9	17.9	28.5
MPA(33%)EVOH32(67%)	187.7	18.7	27.2	216	11.1	7.5	29.7	34.7
EVOH32	189.1	40.8	40.8	–	–	–	40.8	40.8
MPA(83%)EVOH44(17%)	–	0.0	6.3	219.5	23.4	18.7	23.4	25.0
MPA(80%)EVOH44(20%)	–	0.0	7.6	219.8	22.3	17.9	22.3	25.5
MPA(67%)EVOH44(33%)	176.5	0.6	12.6	219.2	19.9	14.9	20.6	27.6
MPA(33%)EVOH44(67%)	182.6	17.1	25.3	215.6	11.9	7.5	29.0	32.7
EVOH44	183.4	37.9	37.9	–	–	–	37.9	37.9
MPA(83%)EVOH48(17%)	–	0.0	5.2	220.1	23.6	18.7	23.6	23.8
MPA(80%)EVOH48(20%)	–	0.0	6.2	218.9	23.9	17.9	23.9	24.1
MPA(67%)EVOH48(33%)	157.1	0.2	10.4	218.5	21.1	14.9	21.3	25.3
MPA(33%)EVOH48(67%)	160.5	14.8	20.7	214.3	12.2	7.5	26.9	28.2
EVOH48	162.9	31.1	31.1	–	–	–	31.1	31.1

<sup>a</sup> A small melting endotherm with a peak temperature of about 92.4°C was found on the thermogram of MPA resin.

220.5°C but significantly lower  $W_c$  value at around 22.4%. Similar to that found in the thermogram of CP specimen, a small melting endotherm with a peak temperature of about 92.4°C was found on the thermogram of MPA resin. Presumably, this melting endotherm is attributed to the melting of the residual traces of CP present in MPA specimen.

After blending varying compositions of EVOH in MPA, the main melting endotherms corresponding to those of the original EVOH and MPA specimens were both found on MPAEVOH thermograms as the weight ratios of MPA to EVOH are equal to or less than 2. However, the peak temperatures associated with the main melting endotherm of MPA and EVOH increase and reduce significantly with increasing the MPA contents present in MPAEVOH resins, respectively, (see Fig. 1 and Table III). On the other hand, it is worth noting that the  $W_c$  values of MPAEVOH specimens are significantly smaller than the summation  $W_c$  values of MPA and EVOH present in MPAEVOH specimens calculated using simple mixing rule. As shown in Table III, the  $W_c$  values of “EVOH-rich phases” of MPAEVOH specimens are slightly smaller than those of pure EVOH specimens present in MPAEVOH specimens calculated using simple mixing rule. However, the  $W_c$  values of “EVOH-rich phases” are dramatically reduced and significantly smaller than those of virgin EVOH specimen present in MPAEVOH specimens calculated using simple mixing rule as the weight ratios of MPA to EVOH are equal to or greater than 2. As shown in Figure 1, the main melting endotherm associated with the EVOH

resins with varying vinyl alcohol contents disappears quickly as the MPA contents present in MPAEVOH increase. In fact, regardless of the vinyl alcohol contents present in the EVOH resins, almost no EVOH melting endotherm can be found on the MPAEVOH thermograms, as the weight ratios of MPA to EVOH reach about 4 (i.e., MPA(80%)EVOH(20%) sample). Under such circumstance, the  $W_c$  values of EVOH-rich phases present in MPAEVOH specimens are roughly equal to zero. In addition, it is worth noting that the  $W_c$  values of EVOH-rich phases increase slightly with increasing the vinyl alcohol contents of EVOH resins present in the MPAEVOH specimens at weight ratios of MPA to EVOH equal to or less than 2 (see Table III). In contrast, the  $W_c$  values of MPA-rich phases present in MPAEVOH specimens are always larger than those of pure MPA crystals present in MPAEVOH specimens calculated using simple mixing rule.

#### Wide angle X-ray diffraction properties of PA, MPA, EVOH, and MPAEVOH specimens

Typical X-ray diffraction patterns of PA, MPA, EVOH, and MPAEVOH specimens are summarized in Figure 2. Similar to the results found in our previous investigations,<sup>23,27</sup> most of the crystals of PA specimen cooled and crystallized at 25°C are  $\gamma$  form crystals,<sup>28,29</sup> which corresponds to a peak diffraction angle at 21.5° shown in their X-ray diffraction patterns. In contrast,  $\alpha$  form PA crystals were found as the main crystals with two diffraction peaks at 20.5° and 24°, when MPA melts were cooled and crystal-

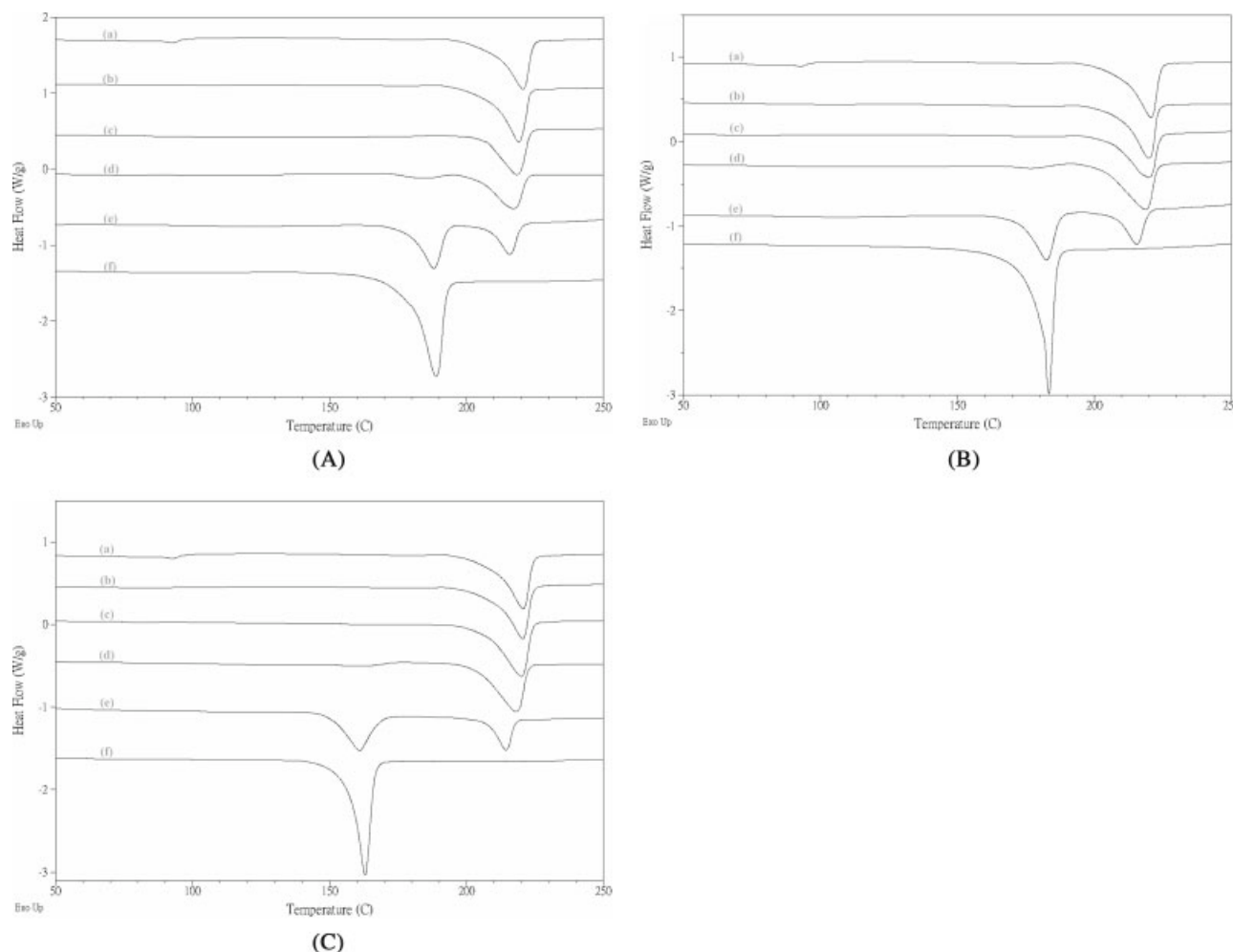


**Figure 1** (A) DSC thermograms of (a) MPA, (b) MPA(83%)EVOH32(17%), (c) MPA(80%)EVOH32(20%), (d) MPA(67%)EVOH32(33%), (e) MPA(33%)EVOH32(67%), and (f) EVOH32 samples scanned at a heating rate of 10 °C/min. (B) DSC thermograms of (a) MPA, (b) MPA(83%)EVOH44(17%), (c) MPA(80%)EVOH44(20%), (d) MPA(67%)EVOH44(33%), (e) MPA(33%)EVOH44(67%), and (f) EVOH44 samples scanned at a heating rate of 10 °C/min. (C) DSC thermograms of (a) MPA, (b) MPA(83%)EVOH48(17%), (c) MPA(80%)EVOH48(20%), (d) MPA(67%)EVOH48(33%), (e) MPA(33%)EVOH48(67%), and (f) EVOH48 samples scanned at a heating rate of 10 °C/min.

lized at 25°C. In fact, the characteristic X-ray diffraction patterns of  $\gamma$  form PA crystals of MPA specimen almost disappear completely (see Fig. 2). These interesting results suggest that the presence of CP in MPA can promote the formation of  $\alpha$  form PA crystals when MPA melts were cooled and crystallized at 25°C. On the other hand, the diffraction patterns of the EVOH specimens can be categorized into two types of lattice forms. The crystals of EVOH32 specimens with 68 wt % vinyl alcohol contents cooled and crystallized at 25°C exhibit a monoclinic lattice diffraction pattern with four peak diffraction angles at 10.8°, 19.8°, 20.2°, and 22.5°, respectively. In contrast, EVOH44 and EVOH48 specimens with lower vinyl alcohol contents (i.e., 52 and 56 wt %) exhibit mainly the orthorhombic crystal lattice with two peak diffraction angles at 20.2° and 21.9°, when they were cooled and crystallized at 25°C. Similar results

were reported by several investigators.<sup>21,30</sup> Cerrada et al.<sup>30</sup> suggest that the type of EVOH crystal lattice formation depends mainly on the cooling rates of the melt and vinyl alcohol contents of the EVOH resins. In their study, EVOH specimens with 68 or 71 wt % vinyl alcohol contents exhibit X-ray diffraction patterns of monoclinic lattice, which are isomorphous to those of polyvinyl alcohol (PVA) resins. However, EVOH specimens with 56 wt % vinyl alcohol contents exhibit orthorhombic X-ray diffraction patterns, which are similar to those of PE resins.

After blending MPA in EVOH resins, the characteristic diffraction patterns of monoclinic and orthorhombic lattices of EVOH crystals become less demarcated with the increasing MPA contents. It is worth noting that regardless of the vinyl alcohol contents present in the EVOH resins, the diffraction patterns of either the monoclinic or orthorhombic

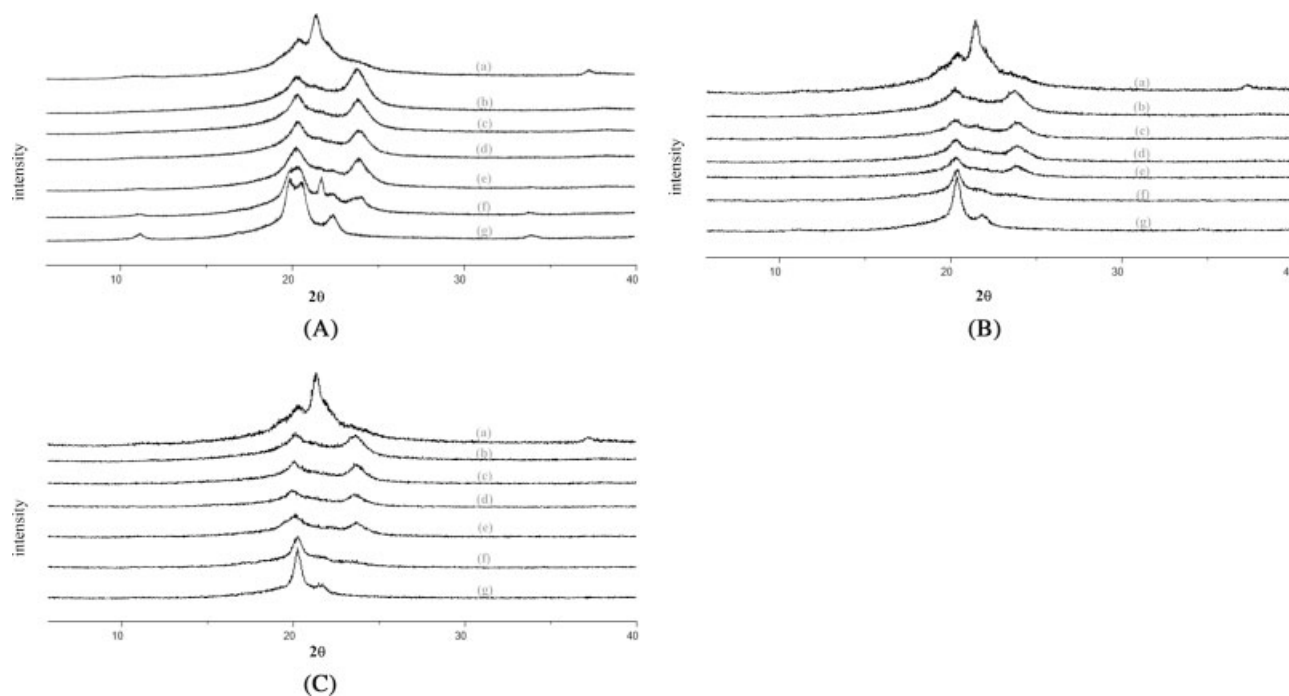


**Figure 2** (A) WAXS diffraction patterns of (a) PA, (b) MPA, (c) MPA(83%)EVOH32(17%), (d) MPA(80%)EVOH32(20%), (e) MPA(67%)EVOH32(33%), (f) MPA(33%)EVOH32(67%), and (g) EVOH32 specimens. (B) WAXS diffraction patterns of (a) PA, (b) MPA, (c) MPA(83%)EVOH44(17%), (d) MPA(80%)EVOH44(20%), (e) MPA(67%)EVOH44(33%), (f) MPA(33%)EVOH44(67%), and (g) EVOH44 specimens. (C) WAXS diffraction patterns of (a) PA, (b) MPA, (c) MPA(83%)EVOH48(17%), (d) MPA(80%)EVOH48(20%), (e) MPA(67%)EVOH48(33%), (f) MPA(33%)EVOH48(67%), and (g) EVOH48 specimens.

lattices of EVOH crystals can be barely found in the MPAEVOH specimens, as the weight ratios of MPA to EVOH of MPAEVOH specimens are more than 2. In fact, the characteristic X-ray diffraction patterns of both monoclinic and orthorhombic lattices of EVOH crystals almost disappear completely (see Fig. 2), when the weight ratios of MPA to EVOH are equal to or greater than 4 (i.e., MPA(80%)EVOH(20%) and MPA(83%)EVOH(17%) samples). Similar to that of MPA specimen,  $\alpha$  form PA crystal is the main crystal present in MPAEVOH specimens regardless of their MPA contents.

These interesting thermal and X-ray diffraction properties suggest that EVOH and MPA are miscible with each other to some extents in MPA-rich and EVOH-rich phases, wherein EVOH molecules interact and are miscible with MPA molecules in the molecular level during the melt blending processes. Presumably, the two main endotherms found in MPAEVOH specimens are mainly attributed to the melting of MPA and EVOH crystals present in the MPA-rich and EVOH-rich phases in MPAEVOH specimens, respectively. However, the presence of MPA and EVOH in MPAEVOH resins can interfere with each other during the course of crystallization, and hence, make both melting peak temperatures of EVOH and MPA reduce significantly with increasing the MPA and EVOH contents, respectively. Moreover, making EVOH molecules “soluble” in MPA-rich phase without phase separation is easier than making MPA molecules

“soluble” in EVOH-rich phase without phase separation. However, EVOH molecules with higher vinyl alcohol contents are likely to have stronger inter and/or intramolecular bondings (e.g., hydrogen bonding) than those with lower vinyl alcohol contents, that can make the EVOH molecules more difficult to disperse in MPA molecules, and hence remain as EVOH-rich phases in MPAEVOH specimens. Presumably, this is the reason why  $W_c$  values and peak melting temperatures of EVOH-rich phases increase slightly with increasing the vinyl alcohol contents of EVOH resins present in the MPAEVOH specimens at weight ratios of MPA to EVOH equal to or less than 2. On the other hand, MPA crystallizes first upon cooling since it has high melt temperature expelling out the amorphous EVOH molecules from the growing crystallization front of EVOH phase, wherein EVOH can be effectively trapped between the crystals of MPA. This might result in inhibition of the crystallization kinetics of EVOH phase occurring at lower temperatures leading to small crystallinity values than those predicted by the simple mixing rule. Presumably, at weight ratios of MPA to EVOH are equal to or greater than 4, most of the EVOH molecules were effectively trapped and crystallization-inhibited between the crystals of MPA during the melt crystallization processes of MPAEVOH specimens. Under such circumstances, the characteristic melting endotherm and X-ray diffraction patterns of EVOH crystals with monoclinic

TABLE IV  
Free-Volume Properties of PE, CP, PA, MPA, and EVOH Samples

Sample	Annihilation intensity $I_3$ (%)	Radius of the average free-volume-cavity $R_f$ (Å)	Average free-volume-cavity size $V_f$ (Å <sup>3</sup> )	Fractional free volume $F_v$ (%)
PE	16.95	3.04	117.73	20.0
CP	21.05	3.02	115.26	24.3
PA	17.19	2.32	52.52	9.0
MPA	17.00	2.45	61.92	10.5
EVOH32	19.11	1.97	32.02	6.1
EVOH44	19.82	2.07	37.09	7.3
EVOH48	20.20	2.11	39.35	8.0

and/or orthorhombic lattices can be barely found in the DSC thermograms and X-ray diffraction patterns of MPA(80%)EVOH(20%) and MPA(83%)EVOH(17%) specimens.

### Free-volume properties

Table IV and Figure 3 summarized the evaluated free-volume properties of PE, MPA, EVOH, and MPAEVOH specimens. As expected, the average radius ( $R_f$ ) and volume ( $V_f$ ) values of the free-volume-cavities of the EVOH and MPA resins are significantly lower than that of the PE resin, wherein the  $R_f$  and  $V_f$  values of the EVOH resins are significantly lower than that of the MPA resin. In addition, the  $R_f$  and  $V_f$  values of EVOH specimens reduce significantly as the vinyl alcohol contents increase. As shown in Table IV and Figure 3(a), the  $R_f$  values of EVOH specimens reduce from 2.11 to 2.07 and then to 1.97 Å, as their vinyl alcohol contents increase from 52 to 56 and then to 68 wt %, respectively, which are significantly smaller than 2.45 and 3.04 Å of the MPA and PE specimen,

respectively. In contrast, the annihilation intensity ( $I_3$ ) values of EVOH specimens are significantly higher than that of the MPA specimen, but reduce consistently with increasing vinyl alcohol contents, in which the  $I_3$  values reflect the relative average numbers of the free-volume-cavities per unit volume [see Fig. 3(b)]. After blending MPA in EVOH, the  $R_f$  and  $V_f$  values of each MPAEVOH sample series tend to increase, as the MPA contents increase, respectively. At a given weight ratio of MPA to EVOH, the beneficial effect of the vinyl alcohol content on reducing the  $R_f$  and  $V_f$  values of MPAEVOH samples persists but become less demarcated as the MPA contents present in MPAEVOH specimens increase. In contrast, the  $I_3$  values of each MPAEVOH sample series tend to reduce with increasing the MPA contents. Similarly, at a fixed weight ratio of MPA to EVOH, the beneficial effect of the vinyl alcohol content on reducing  $I_3$  values of MPAEVOH samples persists at varying MPA contents [see Fig. 3(b)]. On the other hand, regardless of the vinyl alcohol contents present in the virgin EVOH resins, it is worth noting that most  $I_3$  values of each

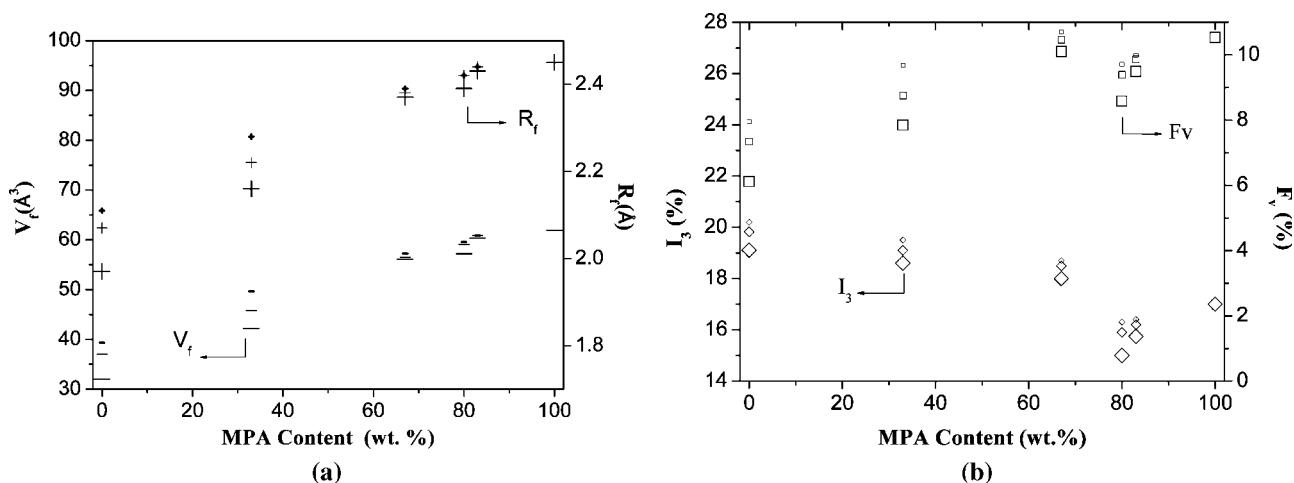


Figure 3 (a) (+) Average radius ( $R_f$ ) and (–) free-volume ( $V_f$ ) values of the free-volume-cavity of MPAEVOH32, MPAEVOH44 and MPAEVOH48 specimens. (The sizes of symbols increase with the increasing vinyl alcohol contents present in virgin EVOH resins.) (b) (◇) annihilation intensity ( $I_3$ ) and (□) fractional free-volume ( $F_v$ ) values of MPAEVOH32, MPAEVOH44, and MPAEVOH48 specimens. (The sizes of symbols increase with the increasing vinyl alcohol contents present in virgin EVOH resins.)

**TABLE V**  
White Spirit Permeation Rates of PE, MPA, EVOH,  
and MPAEVOH Specimens

Specimens	White spirit	
	Permeation rate ( $\times 10^{-3}$ , g/day) <sup>a</sup>	Barrier improvement <sup>b</sup>
PE	300	1
MPA	2.48	121
MPA(83%)EVOH32(17%)	1.85	162
MPA(80%)EVOH32(20%)	0.90	335
MPA(67%)EVOH32(33%)	1.24	241
MPA(33%)EVOH32(67%)	0.82	366
EVOH32	0.34	882
MPA(83%)EVOH44(17%)	2.20	136
MPA(80%)EVOH44(20%)	1.33	226
MPA(67%)EVOH44(33%)	1.52	197
MPA(33%)EVOH44(67%)	1.42	211
EVOH44	1.18	254
MPA(83%)EVOH48(17%)	2.12	141
MPA(80%)EVOH48(20%)	1.44	208
MPA(67%)EVOH48(33%)	1.69	178
MPA(33%)EVOH48(67%)	1.83	164
EVOH48	1.44	208

<sup>a</sup> Permeation rate (g/day) = weight loss of white spirit in 14 days/14days.

<sup>b</sup> Barrier improvement = permeation rate of the specimen/permeation rate of PE specimen.

MPAEVOH sample series are significantly lower than those calculated using simple mixing rule, and hence, a noticeable "negative deviation" was found on the plots of  $I_3$  and fractional free-volume ( $F_v$ ) versus MPA contents as the weight ratios of MPA to EVOH reach about 4.

It is generally recognized that the size and distribution of the free-volume-cavities of polymers are related to the molecular structure and molecular interaction present in their amorphous phases. Strong molecular interaction, such as inter and/or intramolecular hydrogen bondings can attract and hold the polymer molecules in a more condensed way in their amorphous phases and, hence, cause a relatively small  $R_f$  of the free-volume-cavities. Presumably, the significant amounts of OH groups present in EVOH molecules can provide much higher possibility for the formation of intermolecular and/or intramolecular hydrogen bondings in their amorphous regions than those of MPA molecules, although formation of hydrogen bondings between the N—H and C=O groups of the MPA molecules is also possible. In fact, as reported in our recent investigation,<sup>27</sup> an intense broad band centered at approximately  $3330\text{ cm}^{-1}$  corresponding to hydroxyl stretching of a distribution of intermolecular and/or intramolecular hydrogen-bonded OH dimer and multimers was found in the FT-IR spectra of the EVOH specimen. On the basis of these premises, it is reasonable to believe that the average free volumes in the amorphous

regions of the EVOH resins are significantly smaller than that of the MPA polymer and can further reduce with increase in their vinyl alcohol contents. However, after blending MPA in EVOH resin, the presence of MPA molecules can interfere and/or break the hydrogen-bonded hydroxyl groups originally present in EVOH resin, and even form new interaction between carboxyl and hydroxyl groups, as the MPA contents present in MPAEVOH specimens increase. As evidenced by the FT-IR spectra reported in our previous study,<sup>27</sup> the hydrogen-bonded hydroxyl groups of EVOH molecules were broken and turned into free hydroxyl groups gradually with the increasing MPA contents present in MPAEVOH specimens. In fact, most of the hydrogen-bonded hydroxyl groups of EVOH molecules were broken at some optimum MPAEVOH compositions, and the free hydroxyl groups strongly interact with C=O groups of the MPA molecules and blended into MPA-rich phases during the melt blending process. Under such circumstances, the free-volume-cavities originally present in EVOH resin disappeared significantly, and hence, cause the relative average numbers of the free-volume-cavities per unit volume of MPAEVOH resins are significantly lower than those calculated using simple mixing rule, and a noticeable "negative deviation" was found on the plot of  $I_3$  and  $F_v$  versus MPA contents as the weight ratios of MPA to EVOH reach about 4. On the other hand, it is reasonable to understand that, after blending MPA in EVOH resin, the dense molecular structure originally present in the amorphous regions of EVOH specimens was disrupted and changed into sparser structure as the MPA contents increase, although the molecular structures can be hold denser as the virgin EVOH resins are associ-

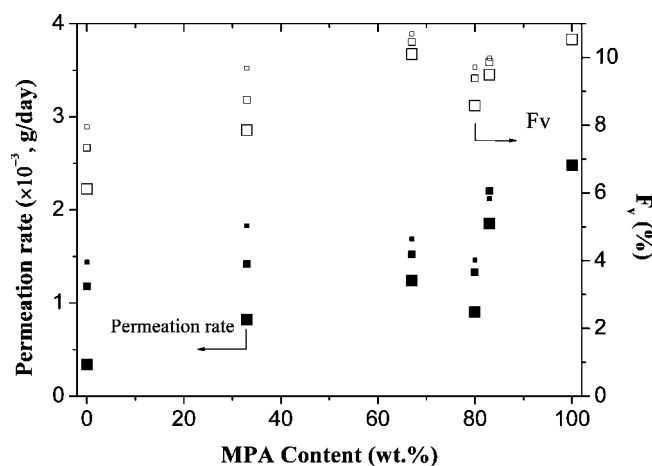


**Figure 4** Comparing (■) barrier properties and (□) fractional free-volumes ( $F_v$ ) of MPAEVOH32, MPAEVOH44, and MPAEVOH48 specimens. (The sizes of symbols increase with the increasing vinyl alcohol contents present in virgin EVOH resins.)



ated with higher vinyl alcohol contents. As a consequence, the average free-volumes of the free-volume-cavities of the MPAEVOH specimens increase significantly as their MPA contents increase, but reduce significantly as the vinyl alcohol contents present in the virgin EVOH resins increase.

#### White spirit permeation properties of hot-pressed sheet specimens

Table V and Figure 4 summarized the white spirit permeation rates of PE, MPA, EVOH, and MPAEVOH hot-pressed sheet specimens prepared in this study. As expected, the PE specimen exhibits the worst white spirit permeation resistance among the base resins (i.e., PE, MPA, and EVOH), wherein all EVOH specimens exhibit even better white spirit permeation resistance than the MPA specimen. In fact, it is worth noting that the barrier resistance of EVOH specimens against white spirit permeation improves significantly as their vinyl alcohol contents increase. As shown in Table V, the white spirit permeation rates of EVOH hot-pressed sheet specimens reduce from 1.44 to 1.18 and then to 0.34 g/day as their vinyl alcohol contents increase from 52 to 56 and then to 68 wt %, respectively, which yield 208, 254, and 882 times of barrier improvement better than that of the plain PE specimen, respectively. After blending varying compositions of EVOH in MPA, the white spirit permeation rates of each MPAEVOH sample series tend to improve as their EVOH contents increase. However, it is interesting to note that a clear "negative deviation" can be found on the plots of the white spirit permeation rates versus MPA contents as their weight ratios of MPA to EVOH present in each MPAEVOH sample series reach about 4. In fact, as shown in Table V, the barrier improvement of MPA(80%)EVOH32(20%), MPA(80%)EVOH44(20%) and MPA(80%)EVOH48(20%) samples against white spirit permeation reach about 335, 226, and 208 times better than that of the PE specimen, respectively, which are significantly better than those of other MPAEVOH specimens (i.e., specimens MPA(33%)EVOH(67%), MPA(67%)EVOH(33%) and MPA(83%)EVOH(17%)) present in their corresponding sample series (see Table V).

It is generally recognized that the molecular composition and structure in the amorphous phase of the polymer can greatly affect its barrier properties, since the permeant molecules are believed to enter and diffuse through the polymer by mostly penetrating through its amorphous regions. It is, therefore, reasonable to suggest that the fractional free-volumes, sizes of the free-volume-cavities and composition in the amorphous regions of the polymers can greatly affect their barrier properties. On the basis of these premises, it is not hard to believe that the small nonpolar white spirit molecules can easily enter into and permeate through the nonpolar amorphous regions of

PE resins with a relatively large  $R_f$  of about 3 Å. In comparison with PE, the presence of the smaller free-volume-cavities, fractional free-volumes and polar functional groups and/or intermolecular hydrogen bondings in the amorphous regions of EVOH and MPA resins, can significantly inhibit the nonpolar white spirit molecules to enter into and permeate through their amorphous regions. Moreover, as shown in the previous section, the  $R_f$ ,  $V_f$ , and  $F_v$  values of EVOH specimens reduce significantly as their vinyl alcohol contents increase. As a consequence, EVOH and MPA sheet specimens exhibit significant better white spirit permeation resistance than PE sheet specimen, wherein the white spirit permeation resistance of the EVOH sheet specimens improve consistently as their vinyl alcohol contents increase. By the same analogy, the white spirit permeation resistance of MPAEVOH resins is expected to improve with the increasing EVOH contents, since the sizes of the average free-volume-cavities ( $R_f$ ,  $V_f$ ) and fractional free-volumes ( $F_v$ ) of the EVOH resins are significantly smaller than those of the MPA resin. However, As shown in Figure 4, in consistent with the MPA content dependence of white spirit permeation rates found earlier, a noticeable "negative deviation" was found on the plots of  $I_3$  and fractional free-volume ( $F_v$ ) versus MPA contents as the MPA contents of each MPAEVOH sample series reach about 80 wt %. These results suggest that the barrier properties of the MPA, EVOH and MPAEVOH specimens are most likely related to the fractional free-volumes ( $F_v$ ) present in their amorphous phases.

#### CONCLUSIONS

The peak melting temperatures and percentage crystallinity ( $W_c$ ) values of the virgin EVOH specimens increase significantly as their vinyl alcohol contents increase. The X-ray diffraction patterns of the melt-crystallized EVOH crystals transform from monoclinic lattice to orthorhombic lattice as their vinyl alcohol contents are equal to or less than 56 wt %. The main melting endotherms and characteristic X-ray diffraction patterns of both monoclinic and orthorhombic lattices of EVOH crystals originally present in MPAEVOH specimens almost disappear completely, as the weight ratios of MPA to EVOH are equal to or greater than 4. Regardless of vinyl alcohol contents, the  $W_c$  values of each MPAEVOH sample series are significantly smaller than the total  $W_c$  values of MPA and EVOH present in MPAEVOH specimens calculated using simple mixing rule, wherein the  $W_c$  values of "EVOH-rich phases" are dramatically reduced and significantly smaller than those of virgin EVOH specimen present in MPAEVOH specimens as the weight ratios of MPA to EVOH are equal to or greater than 2.

However, the  $W_c$  values of EVOH-rich phases increase slightly with increasing the vinyl alcohol contents of EVOH resins present in the MPAEVOH specimens at weight ratios of MPA to EVOH equal to or less than 2. In contrast, the  $W_c$  values of MPA-rich phases present in each MPAEVOH sample series are always larger than those of pure MPA crystals present in MPAEVOH specimens calculated using simple mixing rule. The free-volume properties and white spirit permeation rates of the EVOH specimens reduce significantly as their vinyl alcohol contents increase. A noticeable "negative deviation" was found on the plots of white spirit permeation rates, annihilation intensity ( $I_3$ ) and fractional free-volume ( $F_v$ ) versus MPA contents as the MPA contents of each MPAEVOH sample series reach about 80 wt %. These results suggest that the barrier properties of the MPA, EVOH and MPAEVOH specimens are most likely related to the fractional free-volumes ( $F_v$ ) present in their amorphous phases.

## References

1. Yeh, J. T.; Shih, W. H.; Huang, S. S. *Macromol Mater Eng* 2002, 287, 23.
2. Subramanian, P. M. U.S. Pat. 4, 410, 482 (1983).
3. Subramanian, P. M. U.S. Pat. 4, 444, 817 (1984).
4. Subramanian, P. M. *Polym Eng Sci* 1985, 25, 483.
5. Yeh, J. T.; Fan-Chiang, C. C.; Cho, M. F. *Polym Bull* 1995, 35, 371.
6. Yeh, J. T.; Fan-Chiang, C. C. *J Polym Res* 1996, 3, 211.
7. Yeh, J. T.; Fan-Chiang, C. C.; Yang, S. S. *J Appl Polym Sci* 1997, 64, 1531.
8. Yeh, J. T.; Fan-Chiang, C. C. *J Appl Polym Sci* 1997, 66, 2517.
9. Yeh, J. T.; Jyan, C. F. *Polym Eng Sci* 1998, 38, 1482.
10. Yeh, J. T.; Yang, S. S.; Jyan, C. F.; Chou, S. *Polym Eng Sci* 1999, 39, 1952.
11. Yeh, J. T.; Chao, C. C.; Chen, C. H. *J Appl Polym Sci* 2000, 76, 1997.
12. Yeh, J. T.; Chang, S. S.; Yao, H. T.; Chen, K. N.; Jou, W. S. *J Mater Sci* 2000, 35, 1321.
13. Yeh, J. T.; Chang, S. S.; Yao, W. H. *Macromol Mater Eng* 2002, 287, 532.
14. Yeh, J. T.; Chang, S. S.; Chen, H. Y. *Polym Eng Sci* 2005, 45, 25.
15. Subramanian, P. M. *Polym Eng Sci* 1987, 27, 663.
16. Leaversuch, R.; In *Proceedings of Modern Plastics International*; McGraw-Hill: Lausanne, Switzerland, 1986; p 24.
17. Subramanian, P. M. In *Conference Proceedings—Technical Association of Pulp and Paper Industry; Lamination and Coating Conference* 1984; p 341.
18. Subramanian, P. M.; Mehra, V. *SPE ANTEC* 1986, 1, 301.
19. Diluccio, R. C. U.S. Pat. 4, 416, 942 (1983).
20. Brandrup, J.; Immergut, E. H. *Polymer Handbook*; Wiley: New York, 1989; Chapter 5, p 112.
21. Lagaron, J. M.; Gimenez, E.; Saura, J. J.; Gavara, R. *Polymer* 2001, 42, 7381.
22. Nakanishi, H.; Wang, S. J.; Jean, Y. C. In *Positron Annihilation in Fluids*; Sharma, S. C., Ed.; World Scientific: Singapore, 1988; p 753.
23. Yeh, J. T.; Yao, W. H.; Chen, C. C. *J Polym Res* 2005, 12, 279.
24. Nakanishi, H.; Jean, Y. C.; Smith, E. G.; Sandreczki, T. C. *J Polym Sci Polym Phys Ed* 1989, 27, 1419.
25. Deng, Q.; Sundar, C. S.; Jean, Y. C. *J Phys Chem* 1992, 96, 492.
26. Wang, Y. Y.; Nakanishi, H.; Jean, Y. C.; Sandreczki, T. C. *J Polym Sci Polym Phys Ed* 1990, 28, 1431.
27. Yeh, J. T.; Yao, W. H.; Du, Q. G.; Chen, C. C. *J Polym Sci Polym Phys Ed* 2005, 43, 511.
28. Holmes, D. R.; Bunn, C. W.; Smith, D. J. *J Polym Sci* 1955, 15, 159.
29. Kyotani, M.; Mitsunashi, S. *J Polym Sci Part A-2: Polym Phys* 1972, 10, 1497.
30. Cerrada, M. L.; Perez, E.; Perena, J. M.; Benavente, R. *Macromolecules* 1998, 31, 2559.